Water Dynamics and Structure of Highly Concentrated LiCl Solutions Investigated using Ultrafast IR Spectroscopy

Sean A. Roget, Kimberly A. Carter-Fenk, and Michael D. Fayer*

Department of Chemistry, Stanford University, Stanford, CA 94305 U.S.A.
*Email: fayer@stanford.edu; Phone: (650) 723-4446

Abstract

In highly concentrated salt solutions, the water hydrogen bond (H-bond) network is completely disrupted by the presence of ions. Water is forced to restructure as dictated by the water-ion and ion-ion interactions. Using ultrafast polarization-selective pump-probe spectroscopy (PSPP) of the OD stretch of dilute HOD, we demonstrate that the limited water-water H-bonding present in concentrated lithium chloride solutions (up to 4 waters per ion pair) is, on average, stronger than that occurring in bulk water. Furthermore, information on the orientational dynamics and the angular restriction of water H-bonded to both water oxygens and chloride anions were obtained through analysis of the frequency-dependent anisotropy decays. It was found that the water showed increasing restriction and slowing at frequencies correlated with strong H-bonding when the salt concentration was increased. The angular restriction of the water molecules and strengthening of water-water H-bonds are due to the formation of a water-ion network not present in bulk water and dilute salt solutions. Finally, the structural evolution of the ionic medium was observed through spectral diffusion of the OD stretch using 2D IR spectroscopy. Compared to pure water, there is significant slowing of the biexponential spectral diffusion dynamics. The slowest component of the spectral diffusion, 13 ps, is virtually identical to the time for complete orientation randomization of HOD measured with the PSPP experiments. This result suggests that the slowest component of the spectral diffusion reflects rearrangement of water molecules in the water-ion network.

I. Introduction

The dynamical interactions between water and ions are of fundamental importance to many chemical and biological processes. Water is known to have many unique physical characteristics due to its extensive hydrogen bond (H-bond) network. The solvation of ions reorganizes this network, affecting many of water's properties, including its conductivity, viscosity, molecular diffusion and its ability to solvate molecules such as proteins.[1] Basic knowledge of the effects of ions on the structure and dynamics of water aids in the understanding of a broad range of processes that occur in nature and in the development of new technologies.

For many years, aqueous salt solutions have been examined through a variety of techniques, including Raman,[2] NMR,[3] and dielectric relaxation spectroscopy,[4] X-ray and neutron scattering and molecular dynamics simulations.[5] Of the many experimental techniques, ultrafast IR spectroscopy provides the sensitivity and the time resolution for the measurement of structural dynamics in aqueous salt solutions. Direct observations of the effects of ions on the structure and dynamics of water have been obtained with ultrafast IR experiments through the use of the OD vibrational stretch of dilute HOD, in solution. These experiments provided details on the impact of the cation and anion, specific ion effects, and the range of water-ion interactions in solution.[6-14] Ionic probes such as SCN^-, NO_3^-, and CO_3^- have also been used to examine structural dynamics from the perspective of the ion as well as investigate the formation, and structure of ion pairs and clusters.[15-18]

Highly-concentrated salt solutions have been receiving increasing attention due to their potential use as electrolytes in energy storage devices.[19-21] "Water-in-salt" electrolytes are a safer, more environmentally-friendly alternative to organic solvents used in conventional Li^+-ion batteries, and also have a larger stability window than their dilute "salt-in-water" counterparts.[22-

[24] These electrolytes are typically around 2-3 water molecules per ion pair, and contain an inorganic cation like Li^+, Na^+, or Zn^{2+}, and a larger organic anion.[22-27] Other highly concentrated solutions are also important in chemical processing, e.g., of aluminum, and radioactive waste.[28-30] At these concentrations, the structure of water is very different from that of the bulk liquid. While water typically forms ~4 H-bonds with other water molecules giving rise to a tetrahedral H-bond network,[31-32] in concentrated salt solutions, most of these bonds are dedicated to solvating the ions, completely disrupting the water-water H-bond network. Moreover, there is not enough water to fully solvate the ions, leading to the formation of contact and water-mediated ion pairs and aggregates in solution.[33-34] At extremely high salt concentrations studied here, extended salt/water networks are probably a better description for the ionic system. The nature of highly concentrated salt solutions is profoundly different from dilute solutions, and they are fundamentally interesting and technologically important.

Lithium chloride (LiCl) is an excellent system for investigating concentrated electrolyte solutions as it is a simple halide salt that has a solubility just below 3 water molecules per ion pair. X-ray and neutron diffraction, in combination with molecular dynamics simulations, have been used to examine the restructuring and ion clustering that occur in aqueous LiCl solutions.[5, 34-36] Recently, the structural dynamics of water and ions in aqueous LiCl solutions were observed via two dimensional infrared (2D IR) spectral diffusion experiments on the nitrile stretch of the neutral organic probe, methyl thiocyanate (MeSCN).[37] This required careful analysis of the 2D line shapes from the 2D IR experiment, as MeSCN undergoes chemical exchange processes in addition to its interactions with water and the Li^+ cation, which complicates the extraction of spectral diffusion dynamics from the experiment.[38] Spectral diffusion of the CN stretch of MeSCN showed a component of ~40 ps, which was interpreted as the time for water-ion network

randomization. The CN stretch has strong, well-documented first order Stark coupling.[39-41] The Stark effect and the long nitrile vibrational lifetime makes the spectral diffusion of the CN stretch sensitive to the relatively slow changes in electric fields associated with the water-ion network randomization.

Here, we present a complimentary study to provide direct information on the water structure and dynamics present in concentrated LiCl solutions by looking directly at water through measurements of the OD stretch of dilute HOD. In addition to the spectral diffusion dynamics measured via the 2D IR experiments, direct information on the water reorientation and H-bond structure is obtained from polarization-sensitive pump-probe experiments (PSPP). These experiments reveal additional aspects of the structure and dynamics of the highly concentrated solutions through water H-bond interactions with both water and chloride anions that result in restricted angular motions.

II. Experimental Methods

A. Sample Preparation

Lithium chloride (anhydrous, >99%) was purchased from Sigma-Aldrich and used without further purification. LiCl was stored in a dry-box purged of water vapor until ready for use. LiCl aqueous solutions were prepared in the molar ratios of 1-4, 1-5, and 1-6 LiCl to H_2O. Solutions were also prepared with 5% HOD in H_2O for use in the nonlinear experiments. The solutions were sandwiched between two CaF_2 windows, 1 in. diameter, using a Teflon spacer that was 12 μm thick. Linear IR absorption spectra were measured using a Thermo Scientific iS50 FT-IR spectrometer with a resolution setting of 0.5 cm^{-1}. The chamber of the spectrometer was purged to minimize background absorption of IR active atmospheric gases, such as carbon

dioxide and water vapor. Solutions prepared with H_2O were used to isolate the linear spectrum of the OD stretch in the aqueous salt solutions via background subtraction.

B. Laser System and Nonlinear IR Experiments

The nonlinear experiments were performed using a laser system that has been described previously in detail.[42] Briefly, a Ti:Sapphire oscillator/regenerative amplifier system was used to pump an optical parametric amplifier to generate mid-infrared pulses, centered at ~4 μm with a pulse duration of ~65 fs. The pulses are then split into 2 or 4 pulses and passed through an interferometric system of precision delay stages. The pulses are focused and crossed in the sample using off-axis parabolic reflectors to generate the nonlinear signal of interest. The signal is frequency-resolved and heterodyne-detected using a monochromator equipped with a 32 pixel mercury cadmium telluride array detector configured as a spectrograph.

For the PSPP experiments, the pulse is split into a strong pump pulse and a weaker probe pulse. The pump pulse is linearly polarized +45° relative to the probe pulse, which is horizontally polarized (0°). Immediately after the sample, a computer-controlled polarizer is used to resolve the nonlinear-signal either parallel (+45°) or perpendicular (-45°) to the pump pulse and a second polarizer just prior to the monochromator is used to return the signal polarization to 0°. This polarization scheme enables the detection of the parallel and perpendicular signals in a manner that avoids polarization bias from the diffraction grating in the spectrograph. The parallel and perpendicular signals, $S_{\parallel}(t)$ and $S_{\perp}(t)$, respectively, can be used to obtain the population relaxation, $P(t)$, and the anisotropy, $r(t)$, which is related to the second order Legendre polynomial orientational correlation function, $C_2(t)$, using the following equations:

$$P(t) = [S_{\parallel}(t) + 2S_{\perp}(t)]/3 \tag{1}$$

$$r(t) = \frac{S_{\parallel}(t) - S_{\perp}(t)}{S_{\parallel}(t) + 2S_{\perp}(t)} = 0.4C_2(t) \quad . \tag{2}$$

The relaxation of the vibrational energy absorbed by the OD stretch of HOD also induces an isotropic, long-lived, heating signal in the PSPP experiment. To accurately measure the observables of interest, the heating signal was removed using a well-documented procedure.[43-44]

In the 2D IR experiments, the IR pulse is split into 3 pump pulses and a local oscillator pulse (LO). The 3 pulses are crossed in the box-CARS geometry, generating the nonlinear, echo signal in a distinct, but known, direction. The nonlinear signal is then overlapped with the LO for heterodyne detection. In this experiment, the first two pulses label and store the initial frequencies of the probe molecules. Scanning the time delay, τ, between pulses 1 and 2 produces interferograms at each frequency detected by the array. A numerical Fourier transformation of the interferograms gives data along the horizontal axis, ω_τ, in the 2D spectrum. After a delay, T_w, following the second pulse, the third pulse generates the vibrational echo, which reports the final frequencies of the probe molecules after structural evolution of the system occurs during the T_w period. The spectrograph frequency-resolves the echo/LO pulse, which acts as an experimental Fourier transform that generates the data along the vertical axis, ω_m, in the 2D spectrum. For short T_w periods, the 2D line shape is elongated along the diagonal as the initial frequencies are significantly correlated with the final frequencies. For longer T_w, structural rearrangements in the ionic solution cause decorrelation of the initial and final frequencies, making the 2D line shape rounder. The change in shape with T_w is used to determine the time constants associated with the structural evolution of the system. The center line slope (CLS) method is used to determine the normalized frequency-frequency correlation function, from which the complete FFCF is calculated.[45-47]

III. Results and Discussion

A. Linear Spectra

The OD stretch of HOD in H_2O is sensitive to the wide range of H-bonding configurations present in the water H-bond network, as demonstrated by its broad absorption spectrum shown in Figure 1. Within the vibrational spectrum, stronger and/or more water H-bonds are observed at lower frequencies (red shifted) while weaker and/or fewer H-bonds are observed at higher frequencies (blue shifted). When salt is added, the pure water H-bond network reorganizes to solvate the ions. Water-ion interactions lead to a modification of the OD stretch spectrum. H-bonding between the chloride anion and HOD has a significant effect on the position and width of the spectrum. Anion-associated water populations often appear on the high frequency side of the vibrational spectrum resulting in an overall blue shift. This is the case for chloride because water-chloride H-bonding is weak compared to water-water H-bonding due to the lower charge density of the anion. The effects of H-bonding to halides have been characterized by measuring the absorption spectrum of the OD stretch of HOD in various halide salt solutions. It is observed that the mode shifts more towards higher frequencies as the charge density of the halide ion decreases.[48-50] Notably, fluoride is the only halide anion that leads to a red shift of the OD spectrum.[49-53] Large organic anions, like bistrifilimide (NTf_2^-),[54-55] hexafluorophosphate (PF_6^-),[56-57] and tetrafluoroborate (BF_4^-),[8, 58] which have very diffuse charge, give rise to large spectral shifts to higher frequency, > +100 cm^{-1}, compared to the OD stretch in bulk water absorption spectrum which is peaked at 2509 cm^{-1}. It was also found that the cation has a role in determining the OD stretch spectrum, though it is a more subtle effect.[13]

The absorption spectra of the OD stretch of HOD in concentrated LiCl solutions are shown in Figure 1. The small features around 2350 cm^{-1} are due to trace atmospheric CO_2

remaining in the FT-IR sample compartment. As salt is added to the solution, the OD stretch spectrum increasingly shifts from 2509 cm^{-1} to 2527 cm^{-1}. The shift is caused by the presence of water interacting with chloride anions (chloride-associated population), which arises from the solvation of LiCl. As the concentration of LiCl increases, the center of the overall spectrum approaches the center of the chloride-associated spectrum, as it becomes a larger fraction of the water H-bonding interactions. This is shown in Figure 1, where the concentration increases from bulk water to an intermediate concentration, 1-16, and then to high concentrations. The 1-6 to 1-4 concentrations are virtually identical, though the 1-4 concentration shows very slight narrowing on the wings of the spectrum.

When there is a large spectral shift caused by the water-anion H-bonding interaction, the anion-associated spectrum can be resolved from the water-associated spectrum and its characteristics determined through peak fitting. However, due to the small spectral shift caused by the chloride anion, demonstrated by the ~20 cm^{-1} shift in the overall spectrum at the highest concentrations, it is not possible to separate the anion-associated spectrum using the linear spectra. To resolve the water-chloride and water-water spectral features, the differences in the vibrational lifetimes of the two species were employed, as described in the next section.

B. Vibrational Relaxation

The population decays calculated from the PSPP experiments (Eq. 1) are measurements of the vibrational relaxation of the probe molecule to the ground state following excitation. The vibrational lifetime is a measure of how quickly the energy absorbed by the vibrational mode is dissipated into lower energy intramolecular and bath modes.[59] Vibrational relaxation is thus sensitive to the coupling of the probe to its surrounding environment. If there are distinct local

interactions between the probe and the medium, then there can be differences in the coupling of the vibrational energy to the bath, giving rise to multi-exponential population decays.

The normalized frequency-dependent population decays of the OD stretch of HOD in 1-5 LiCl solution are shown in Figure 2. The vibrational relaxation at each frequency fits well to a biexponential decay, indicating that there are two distinguishable populations present in the salt solution. The two decay components are from the presence of both water-water and water-chloride H-bonding as discussed in the previous section. The lifetimes of these populations for the different concentrations are provided in Table 1. Based on previous findings, the fast component can be attributed to the water-associated population, while the slow component is the chloride-associated population.[6, 12-13] The longer time constant reflects a weaker coupling of the OD stretch vibrational mode to the medium and is much longer than observed in pure water. In the more extreme case of very dilute water (isolated water molecules) in a room-temperature ionic liquid, the lifetime of the anion-associated water is tens of picoseconds.[54] With increasing concentration of salt, there is an observable increase in the lifetime of the anion-associated population, while the lifetime of the water-associated population was observed to be independent of the concentration for the concentrations studied but slightly faster than the lifetime of HOD in bulk water.

The frequency-dependent amplitudes determined from the biexponential fits are shown in Figure 3. These amplitudes map out the contributions of the water-water and water-anion H-bonds to the overall OD stretch absorption spectrum. The amplitudes are normalized to the maximum value of the overall pump-probe signal, similar to the normalized linear spectra in Figure 1. Due to the difference of the vibrational lifetimes of the two species, the overlapping contributions can be separated into individual component spectra, that is the lifetime amplitude

spectra (LAS). The frequency range of the LAS is limited at the lower frequencies due to the presence of the 1-2 transition, which is a result of excited state absorption in the third-order nonlinear experiment. In contrast, the 0-1 transition is a result of ground state bleach and stimulated emission. Therefore, these two transitions occur with opposite signs and cancel each other where they overlap in frequency. Moreover, the 0-1 and 1-2 transitions relax with the same vibrational lifetime, thus, they cannot be resolved through multi-exponential fitting.

As noted in the previous section and shown in Figure 3, the water-chloride population (with the longer lifetime) is shifted to higher frequencies compared to bulk water due to weaker H-bonding between water and the chloride anion. A Gaussian fit to the water-chloride spectrum indicates that it is centered at 2530 cm^{-1}, slightly higher than the center of the total linear absorption spectrum (Figure 1). The shape of the water-chloride spectrum is largely unchanged with concentration, though, like the linear spectra, the highest concentration has some narrowing on the wings of the transition. It is also observed that the water-water spectrum is shifted to lower frequencies (2492 cm^{-1}), compared to bulk water (2509 cm^{-1}) and the shape and position remain virtually identical for the concentrations studied. The water-water component of the 1-5 LiCl solution is compared to the frequency-dependent amplitudes from population decays of HOD in bulk water in Figure 4. The spectral shift of the water-water population in the salt solutions indicates that the H-bonding interaction is stronger, on average, than that observed in bulk water. A red shift also occurs when a water hydroxyl H-bonds to a fluoride anion, though the shift is even larger for fluoride. The fluoride-associated population shows a spectral shift of the OD stretch, which is ~ –60 cm^{-1} (~2450 cm^{-1}).[51-52] This frequency shift is often attributed to fluoride being “structure-making” ion in the Hofmeister series, whereas the other halides are borderline, if not “structure-breaking” ions. However, since the red shift is observed in the water-

associated population of the LiCl solution, the enhanced H-bond strength is more comparable to the water interactions found in ice, which has a highly ordered H-bond network.[60-61]

Molecular dynamics (MD) simulations have indicated that in highly concentrated LiCl solutions, there are many contact ion pairs and clusters as well as solvent-shared and solvent-separated ion pairs.[5, 34-35] (While the term clusters is frequently used in the literature, there is a continuous network of water and ions with different local arrangements.) Thus, it can be concluded that the frequency shift of the water-water spectrum is due to the formation of larger water-ion structures that foster stronger interactions between the water molecules. Most of the water-water interactions that occur in these solutions are of the form of solvent-separated ion pairs, where two water molecules act as the bridge between oppositely-charged ions. Formations such as these can possibly strengthen an H-bond by increasing the partial charges of the H-bond donor and acceptor through electrostatic interactions between the water lone pairs and the ions. Evidence of such interactions was found in recent classical MD simulations, where strengthening of the H-bond shared between water molecules in the first and second solvation shell of ions was observed when the H-bond donor is directly interacting with the cation or the H-bond acceptor is directly interacting with an anion.[62]

C. Orientational Relaxation

The anisotropy calculated from the PSPP experiments, as described in Eq. 2, is a measure of the water orientational dynamics. It is proportional to the second order Legendre polynomial orientational correlation function, $C_2(t)$, which describes the decorrelation of the orientation of the transition dipole (OD bond vector) as the probe reorients in angular space. At time, $t = 0$, the initial anisotropic orientational distribution of OD bonds excited by the pump pulse and their final orientations are perfectly correlated, giving an anisotropy value of 0.4. As time proceeds,

the OD bonds reorient, leading to complete decorrelation once the ensemble of HOD molecules has sampled all angles, corresponding to an anisotropy value of 0. Although the OD bond direction is measured in the experiment, orientational relaxation requires reorientation of the entire HOD molecule. In the bulk liquid, water reorients via jump reorientation, which involves the concerted rearrangement of many water molecules.[63] While the OD vibrational frequency and lifetime are principally determined by the interactions of the OD, the reorientation of HOD is more global, likely involving multiple ions and water molecules.

The anisotropy decays of HOD in the various LiCl solutions near the center frequency are shown in Figure 5. The experimental data begins at ~250 fs because the finite pulse duration of the overlapping pump and probe pulse generates a strong, non-resonant signal from the sample that obscures the data at short time delays. The frequency-dependent anisotropy decays of each concentration were fit to biexponential functions, sharing the time constants across all frequencies. Fitting the decays at each frequency individually yielded time constants that were the same within experimental error. The results of the curve fitting are given in Table 2. When the fits are extrapolated back to $t = 0$, the decays begin slightly below 0.4. This is due to fast inertial motions (<100 fs) of the water molecules, which have time dependence that cannot be experimentally resolved because of the pulse duration.[64]

The orientational relaxation of HOD in bulk water fits well to a single exponential decay with a reorientation time constant of 2.6 ps.[6, 44] In the salt solutions, the orientational dynamics are much slower than observed in bulk water and have two timescales for reorientation. These two time constants can be understood using the wobbling-in-a-cone model.[65-67] The first time constant, t_1, describes reorientation in a restricted angular space defined by a cone of half-angle, θ_c. The second, longer time constant, t_2, describes the complete angular diffusion occurring

following the release of constraints that restricted the short time angular motion. The second time constant corresponds to the time for complete randomization of the transition dipole direction. When wobbling-in-a-cone dynamics occur, the orientational correlation function is given by:

$$C_2(t) = [S_2^2 + (1 - S_2^2)\exp(-t / t_c)]\exp(-t / t_m) \quad (3)$$

where, t_c is the restricted (cone) angular diffusion time constant, t_m is the final complete angular diffusion time constant, ($t_m = \frac{1}{6D_m}$, where D_m is the orientational diffusion constant), and S_2 is the generalized order parameter given by:

$$S_2 = \frac{1}{2}\cos\theta_c(1 + \cos\theta_c)\,. \quad (4)$$

The orientational correlation time constants in the wobbling-in-a-cone model are related to the time constants t_1 and t_2 of the biexponential decay by $t_c = (t_1^{-1} - t_2^{-1})^{-1}$ and $t_m = t_2$. The restricted angular diffusion constant, D_c, depends on both t_c and θ_c and can be described for $\theta_c < 30°$ by,

$$D_c \cong \frac{7\theta_c^2}{24t_c}\,. \quad (5)$$

In the results presented, the full expression for any cone angle is used to calculate the diffusion constant as described in the literature, although the differences from the use of Eq. 5 are negligible.[67]

For the concentrations studied, the time constants from the biexponential fit to the anisotropy do not vary, giving a wobbling time, t_c = 2 ps and a free diffusion time constant, t_m = 12 ps. The free diffusion reorientation is noticeably slower than in bulk water, which is in line with previous measurements of aqueous salt solutions.[6, 12-13] Even though the time constants are essentially identical at each concentration, it is evident that there are differences in the shapes of the decays caused by changes in the wobbling cone angle, θ_c, with concentration. The frequency-

dependent cone angles are presented in Figure 6. As the salt concentration is reduced, there is an overall increase in the cone angles across all frequencies, implying that there is more freedom to reorient at short time when the H-bonds are intact for the more dilute salt solutions. Figure 6 also shows that the frequency dependence of the cone angles vary with concentration. The change in cone angles with frequency is well described by a linear fit. As the concentration decreases, the slope of the cone angles with frequency also decreases. The time constants and diffusion constants are given in Table 2 as well as the average cone angle and the slope for each LiCl solution.

As described in the previous section, the frequency is correlated to the strength of the OD bond. At the highest concentration studied, there is a wide range of cone angles observed for different H-bond strengths, with the ODs with strong H-bonds (lower frequencies) being more restricted than those with weaker H-bonds. As the concentration decreases (see Fig. 6), there is a much smaller range of angles, decreasing from ~7° for the 1-4 concentration to ~3° for the 1-6 concentration over the same frequency range (range of H-bond strengths). Furthermore, since t_c is frequency-independent, the diffusion constant, D_c, follows the same trends (see Eq. 5); there is a wider range of cone orientational diffusion constants at higher concentration, with smaller diffusion constants observed for stronger H-bonds. At lower concentrations, the cone orientational diffusion constants vary much less with H-bond strength (frequency).

Though wobbling-in-a-cone dynamics have been reported for HOD in a range of salt solutions,[6, 12-13, 19] frequency-dependence of the cone angles has not been reported for simple salt solutions. Most simple salts have limited solubility, so it is possible that the large frequency-dependence observed here, which becomes relatively small by 1-6 molar ratio, may not have been present in previous studies. A wide range of cone angles has been observed for 1-2.5

$LiNTf_2$ solution (ion pairs per H_2O) and 1-0.66 $EmimNTf_2$ ionic liquid in agreement with the 1-4 LiCl results presented here, but no concentration-dependent studies were performed.[55] These results suggest that it is possible that the frequency dependence is present for other highly concentrated salt solutions. For 1-alkyl-3-methylimidazolium tetrafluoroborate ionic liquids of various alkyl chain lengths, while there was strong variation in the cone angle across frequency, it was observed that the ratio of ion pairs to water did not have a significant effect on the frequency dependence.[58]

The concentration dependence indicates that the H-bond strength is not the only factor determining the cone angle. Another possible factor is steric hindrance in the salt solution from structural ordering induced by the high concentration of salts. Previous PSPP experiments of molecular probes confined in the free volume elements of amorphous polymers have been used to determine the size distribution of the free volume regions based on the variation of the cone angles.[68-69] Though water is not "confined" in a given space as in the polymers, it is not hard to visualize water angularly constrained by structural features such as ion crowding at these high concentrations. The simplest examples are water involved in solvent-shared and separated ion pairs. When acting as a bridge between Li^+ and Cl^- ions, water would be expected to be highly constrained, resulting in slow reorientation. The observed restructuring of the solution appears to have a large effect on the angular space available for water molecules undergoing strong H-bonding interactions. The observed restriction of the cone angles is likely due to the formation of extended water-ion network structures (extended aggregation) rather than ion pairs since MD simulations indicate that there is a significant number of ion pairs even at the lowest concentration studied here. At the high concentrations studied here, ion pairs will not exist in

isolation surrounded by water, but rather as one component of an extended system of water-ion configurations.

D. Spectral Diffusion

Spectral diffusion is the fluctuation of the vibrational frequencies of probe molecules' vibrational transition due to structural evolution of their surrounding environment. From the 2D IR experiment (described in Section III), spectral diffusion dynamics can be measured from the time dependence of the 2D vibrational spectra. The change in shape of the 2D spectrum with T_w can be seen in Figure 7, which displays 2D spectra of the OD stretch of HOD in 1-5 LiCl solution at two times, T_w = 1 and 10 ps. In the figure, the red band along the diagonal (dashed line) corresponds to the 0-1 vibrational transition (which is generally used for analysis), while the blue band that is off-diagonal arises from the 1-2 transition. The time dependence of the spectral diffusion is obtained from analysis of the shape change of the 2D spectrum with T_w. This analysis is done using the CLS method, which gives the normalized frequency-frequency correlation function (FFCF).[45-46] The FFCF obtained from analysis is the probability that the vibrational probe at an initial frequency (ω_τ) is at the same frequency at a later time (ω_m), averaged over all probe molecules. The CLS(T_w) begins at 1 and decays to zero at sufficiently long time due to the time evolution of the probe frequencies caused by spectral diffusion (structural evolution).

The complete FFCF is typically described using the Kubo model:[70-71]

$$\text{FFCF}=C_\omega(t)\langle\delta\omega(0)^2\rangle=\langle\delta\omega(t)\delta\omega(0)\rangle=\sum_i \Delta_i^2 \exp[-t/\tau_i] \quad (5)$$

where, $\delta\omega(t)=\omega(t)-\langle\omega\rangle$ is the frequency fluctuation as a function of time, Δ_i is the frequency fluctuation amplitude, and τ_i is the decay time constant for the i^{th} component of the frequency

fluctuations. The homogeneous linewidth, $\Gamma = \frac{1}{\pi T_2}$, which has contributions from ultrafast dephasing processes as well as the vibrational lifetime and the orientational relaxation, can also be observed as the deviation of the CLS(0) value from 1. In the limit $\Delta_i \tau_i \ll 1$, the i^{th} component is motionally-narrowed and contributes to the homogeneous linewidth. Homogeneous dephasing in water systems usually dominates the homogeneous linewidth. By using both the CLS(T_w) decay and the linear absorption spectrum, the complete FFCF, including the homogeneous linewidth can be determined.[45-46, 72]

The CLS(T_w) decays of the OD stretch of HOD in the LiCl solutions are shown in Figure 8. These decays effectively reflect the spectral diffusion of the chloride-associated population, because, as indicated by the population amplitudes (Fig. 3) and the short lifetime (~1.2 ps), the water-associated population only makes a small contribution to the 2D IR signal. In addition, the CLS analysis is performed on data around the peak of the 2D spectrum, which is further dominated by the chloride-associated population. Chemical exchange between the two populations is possible, which would result in the growth of off-diagonal peaks, and has been seen in 2D IR experiments of HOD in perchlorate and BF_4^- salt solutions.[8-9] However, there is no evidence of off-diagonal peak, suggesting that the exchange processes occur on a timescale too long to be observed in the experiments. A biexponential function provides the best fits to the CLS(T_w) decays, demonstrating that spectral diffusion occurs via two structural processes. The parameters for the full FFCF were calculated based on the fits and are presented in Table 3.

The CLS(T_w) decay of HOD in bulk water also has two decay components with time constants of 0.4 and 1.7 ps (also presented in Table 3). Molecular dynamics simulations have shown that the fast time constant is mainly a result of fluctuations in the H-bond length with some contributions from angular fluctuations, while the slower time constant is a result of

breaking and making H-bonds, which leads to complete randomization of the H-bond network.[73-74] With the addition of LiCl, it is likely that the structural processes remain the same but they are much slower, with a fast component of 1.2 ps and a slow component of 13 ps. The slowing of the spectral diffusion in concentrated LiCl solutions compared to pure water dynamics are in line with previous measurements of HOD in lower concentration aqueous salt solutions.[6, 13] The time constants for the LiCl solutions are independent of concentration within experimental error, and the main difference between solutions is the amplitude of each component of the overall decay as quantified by the Δ_is presented in Table 3. It is worth noting that the slow component of the anisotropy (Table 2) and the slow component of the CLS decay (Table 3) are essentially the same within experimental error. Though the FFCF and $C_2(t)$ are different correlation functions, the same dynamical process, i.e. the breaking and making of H-bonds and jump reorientation, is responsible for the decays in bulk water. The dynamical observables measured using the two experiments are not necessarily the same. For example, HOD in bulk water has reorientation time of 2.6 ps while its slowest spectral diffusion time constant is 1.7 ps. 2D IR experiments on HOD in lower concentration salt solutions than those studied here, also display spectral diffusion times that are faster than the reorientation time.[13] In bulk water, while orientational relaxation requires jump reorientation, spectral diffusion can occur through the rearrangement of H-bonds of surrounding water molecules bonded to the HOD, which change the strengths of the H-bonds, and therefore the frequency of the OD, without the HOD molecule itself undergoing jump reorientation. In a similar vein, recent simulations show that a component of spectral diffusion is associated with breaking an H-bond and then reforming the same H-bond.[75] Though, if an H-bond to HOD breaks and reforms without the other associated water molecules changing their configurations, there would be no frequency change. The virtually identical slowest components

of the spectral diffusion and orientational relaxation timescales measured here may be an indication that, in these very high concentration salt solutions, the slow spectral diffusion is dominated by reorientation.

Spectral diffusion dynamics of aqueous LiCl solutions over the same range of concentrations were recently measured using the nitrile stretch of MeSCN.[37] This probe was shown to be a good reporter of the water spectral diffusion, reproducing the bulk water spectral diffusion time constants.[38] The spectrum of the CN stretch is very narrow (~20 cm^{-1}) and has two peaks, one that arises when water is bound to the N lone pair and the other when Li^+ is bound. The CN stretch vibrational lifetime is long, ~30 ps, allowing the observation of chemical exchange, i.e., water replacing the Li^+ bound to N and Li^+ replacing water. The time constants for water replacing Li^+ range from 92 ps to 154 ps as the concentration is decreased from 1-4 to 1-6, and for Li^+ replacing water go from 42 ps to 59 ps.[38]

There are significant differences between the spectral diffusion measured using the CN stretch of MeSCN and the OD stretch of HOD as vibrational probes. The MeSCN probe reported three spectral diffusion decay processes.[37] The first two decay components were thought to be slower versions of the spectral diffusion processes observed in bulk water. While the first time constant (~1.2 ps) is very similar for the CN and OD probes, the second time constant is significantly longer for HOD,~13 ps, than it is for MeSCN, 4 ± 1 ps. In addition, MeSCN reported a third, long time component of ~40 ps that was not observed with HOD. Within experimental error, the CN spectral diffusion was the same whether water or Li^+ was bound to the N lone pair. The error bars for the CN results were large enough that, regardless of the concentration or which species was bound to the N lone pair, the dynamics all overlapped. The orientational relaxation times of MeSCN range from ~15 ps to ~8 ps as the concentration is

reduced from 1-4 to 1-6 with water bound and from ~54 ps to ~36 ps when Li^+ is bound.[38] Again, the ~4 ps spectral diffusion time for the CN is independent of concentration and whether water or Li^+ is bound to the CN. Therefore, orientational relaxation is not responsible for the spectral diffusion.

A major difference between the interactions of the CN probe and the OD probe with their surroundings is that CN displays a strong, well-documented first order Stark effect.[39-41] Electric fields produced by the medium have a major effect on the vibrational frequencies of the nitriles. In contrast, the frequencies of OD hydroxyl moieties are dominated by the H-bond interactions. For CN, the first spectral diffusion component is likely caused by the H-bond length fluctuations of the species bound to the N lone pair (water or Li^+). For the OD of HOD, fluctuations of the H-bond to the chloride cause this component of the spectral diffusion. For the second component, fast fluctuations of the sea of ions and water surrounding the MeSCN produce fast electric field fluctuations, which in turn produce frequency fluctuations through first order Stark coupling. The inhomogeneous distribution of electric fields will contribution to the portion of the inhomogeneous broadening (Δ_2) associated with the ~4 ps time scale. Interactions with the MeSCN other than the Stark coupling can also contribute to Δ_2. Simulations of $SeCN^-$ in bulk water showed that interactions with water in different orientations about the CN bond contributed to inhomogeneous broadening and spectral diffusion.[76] The combined fluctuations of the Stark effect and other interactions can result in the ~4 ps spectral diffusion time, τ_2. In contrast, the frequency of the OD of HOD H-bonded to chloride is mainly sensitive to the H-bonding configuration. Jump reorientation will break and remake new H-bonds producing frequency changes, which occur on a timescale of 13 ± 1 ps.

The CN stretch of MeSCN has a much longer lifetime (~30 ps) than the OD stretch of HOD (~5 ps). Could the triexponential decay of the CN FFCF compared to the biexponential decay for the OD be caused by the short OD lifetime preventing the observation of a longer time scale spectral diffusion component? We found that the inclusion of a third slow component in the CLS decay of HOD or an offset, did not improve the fit to the data. The Aikaike statistical test was used to determine if a triexponential function produced a statistically significant improvement in the fit compared the biexponential decay. The results showed that the biexponential fit is substantially preferred over the triexponential model.

The third time constant found using the CN probe is ~40 ps and is independent of concentration within the relatively large error bars.[37] The ~40 ps component was ascribed to first order Stark coupling to the fluctuating electric fields produced by the water-ion network, implying that this is the time constant for the complete randomization of the network. As mentioned above, and shown in several simulations studies,[77-79] other types of intermolecular interactions in addition to Stark coupling can contribute to inhomogeneous broadening and spectral diffusion. Here, we compared spectral diffusion measured by two vibrational probes in the identical LiCl solutions, MeSCN, which has strong first order Stark coupling and HOD, which does not. The absence of the long time constant from the decays observed with HOD supports the assignment[37] of the long time component of the MeSCN spectral diffusion to the randomization of the water-ion network.

IV. Concluding Remarks

We have investigated the effects of very high LiCl concentrations on the structure and dynamics of water in salt solutions through the use of the OD stretch of isotopically dilute HOD as a vibrational probe. At these high concentrations, the presence of ion pairing and clustering is

significant, resulting in a continuous network of water-ion structures. This structural organization produces substantial changes in the properties of the medium compared to bulk water and low concentration salt solutions.

Vibrational relaxation, which is sensitive to the coupling of the vibrational mode of the OD probe to its local environment, was used to separate the OD stretch absorption spectrum into contributions from water-water and water-anion interactions. Through this separation, the average H-bond strength of these interactions can be determined from the center frequency of the corresponding spectra. While the chloride-associated water population (OD H-bonded to chloride) was shifted to higher frequencies (weaker H-bonds than bulk water), in agreement with previous experiments, it was found that the water-associated population (OD H-bonded to a water oxygen) was notably shifted to lower frequencies, indicating that the water-water H-bond interaction in concentrated LiCl solutions is on average stronger than those in bulk water. The enhanced H-bond strength of these interactions, in response to the high salt content in solution, has an impact on water's properties such as viscosity and diffusion. The configuration of the LiCl ions near the interacting water molecules affect the partial charges of the H-bond donor and H-acceptor in a manner which strengthen the H-bonds.[62]

Through careful analysis of the anisotropy from the PSPP experiments, reorientation dynamics and angular restriction about the intact water H-bond were observed. At the high LiCl concentrations studied, it was found that there is a wide range of dynamics and angular restrictions, which vary with the OD stretch frequency. The dynamics and restrictions were quantified using the wobbling-in-a-cone model, which gave the restricted diffusion constants and wobbling cone angles. More strongly H-bonded water molecules showed much slower diffusion and more angular restriction. The magnitude and frequency dependence of the restrictions

decreased as the molar ratio was reduced from 1-4 to 1-6, becoming almost frequency-independent at the lower concentration. These observations can be rationalized as increasing steric hindrance with increasing salt concentration caused by more structural ordering. The wobbling cone angles increase at all frequencies studied as the water content increases, probably as a result of structures less crowded with ions. The stiff structures imparted by the ions have a particularly notable effect on more strongly H-bonded waters, similar to the results obtained from the vibrational relaxation measurements.

Spectral diffusion dynamics (structural fluctuations) sensed by the OD stretch of HOD in the LiCl solutions were also measured using 2D IR spectroscopy. In bulk water, spectral diffusion arises on a very fast time scale most likely from the local fluctuations of the H-bond length and on a slower time scale from breaking and making H-bonds leading to the complete randomization of the water H-bond network. In the LiCl solutions, these processes are significantly slower than in bulk water and dilute salt solutions. While the time constants for the two processes showed no change with salt content within experimental error at these high concentrations, the frequency fluctuation amplitudes indicated that the H-bond reorganization plays a more dominant role in the inhomogeneous broadening of the vibrational mode as the salt concentration increases. The slowest component of the spectral diffusion, ~13 ps, is essentially identical to the time for complete orientational relaxation measured with the PSPP anisotropy decay measurements. The near identity of the slowest component of the spectral diffusion and the time for complete orientational relaxation suggests that this spectral diffusion component reflects rearrangement of water molecules in the water-ion network.

In summary, we have provided detailed insights into the influence of water-ion networks on the dynamics and structure of water in very concentrated LiCl solutions. These experiments

provide a step toward understanding water-ion, ion-ion, and water-water interactions in water-in-salt electrolytes. Previous experiments and simulations on specific cations and anions have reported trends in the angular restriction and the enhancement of the H-bond strength.[12-13, 62] However, the frequency dependence of the cone angles and the H-bond strength at high concentrations have not been thoroughly investigated. In future experiments, the concentration range of LiCl will be extended and *ab initio* MD simulations (currently in progress) will be used to obtain increased molecular level information on structure and dynamics. The experiments and simulations will also be applied to other ionic systems.

Associated Content

Author Information

Corresponding Author

Professor Michael D. Fayer
Department of Chemistry
Stanford University
Stanford, CA 94305-5080
orcid.org/0000-0002-0021-1815
Email: fayer@stanford.edu

Authors

Sean A. Roget
Department of Chemistry
Stanford University
Stanford, CA 94305
orcid.org/ 0000-0003-2470-3571

Kimberly A. Carter-Fenk
Department of Chemistry
Stanford University
Stanford, CA 94305
orcid.org/ 0000-0003-0071-7127

Complete contact information is available at:

https://pubs.acs.org/xxxxxxxxx

Notes

The authors declare no competing financial interest.

Acknowledgments

This work was supported by the National Science Foundation, Division of Chemistry, Award Number 1954392.

References

1. Marcus, Y., Effect of Ions on the Structure of Water: Structure Making and Breaking. *Chem. Rev.* **2009,** *109*, 1346-1370.

2. Terpstra, P.; Combes, D.; Zwick, A., Effect of salts on dynamics of water: A Raman spectroscopy study. *J. Chem. Phys.* **1990,** *92*, 65-70.

3. Chizhik, B. V. I., NMR relaxation and microstructure of aqueous electrolyte solutions. *Mol. Phys.* **1997,** *90*, 653-660.

4. Cota, R.; Ottosson, N.; Bakker, H. J.; Woutersen, S., Evidence for Reduced Hydrogen-Bond Cooperativity in Ionic Solvation Shells from Isotope-Dependent Dielectric Relaxation. *Phys. Rev. Lett.* **2018,** *120*, 216001.

5. Harsányi, I.; Pusztai, L., Hydration structure in concentrated aqueous lithium chloride solutions: A reverse Monte Carlo based combination of molecular dynamics simulations and diffraction data. *J. Chem. Phys.* **2012,** *137*, 204503.

6. Park, S.; Fayer, M. D., Hydrogen bond dynamics in aqueous NaBr solutions. *Proc. Nat. Acad. Sci. U.S.A.* **2007,** *104*, 16731-16738.

7. Bakker, H. J., Structural Dynamics of Aqueous Salt Solutions. *Chem. Rev.* **2008,** *108*, 1456-1473.

8. Moilanen, D. E.; Wong, D.; Rosenfeld, D. E.; Fenn, E. E.; Fayer, M. D., Ion-water hydrogen-bond switching observed with 2D IR vibrational echo chemical exchange spectroscopy. *Proc. Nat. Acad. Sci. U.S.A.* **2009,** *106*, 375-380.

9. Ji, M. B.; Odelius, M.; Gaffney, K. J., Large Angular Jump Mechanism Observed for Hydrogen Bond Exchange in Aqueous Perchlorate Solution. *Science* **2010,** *328*, 1003-1005.

10. Tielrooij, K. J.; van der Post, S. T.; Hunger, J.; Bonn, M.; Bakker, H. J., Anisotropic Water Reorientation around Ions. *J. Phys. Chem. B* **2011,** *115*, 12638.

11. Tielrooij, K. J.; van der Post, S. T.; Hunger, J.; Bonn, M.; Bakker, H. J., Cooperativity in Ion Hydration. *J Phys Chem B* **2011,** *115*, 12638-12647.

12. Post, S. T. v. d.; Bakker, H. J., The combined effect of cations and anions on the dynamics of water. *Phys. Chem. Chem. Phys.* **2012,** *14*, 6280-6288.

13. Giammanco, C. H.; Wong, D. B.; Fayer, M. D., Water Dynamics in Divalent and Monovalent Concentrated Salt Solutions. *J. Phys. Chem. B* **2012,** *116*, 13781-13792.

14. Wei, Q.; Zhou, D.; Bian, H., Negligible cation effect on the vibrational relaxation dynamics of water molecules in NaClO4 and LiClO4 aqueous electrolyte solutions. *RSC Advances* **2017,** *7*, 52111-52117.

15. Bian, H.; Wen, X.; Li, J.; Chen, H.; Han, S.; Sun, X.; Song, J.; Zhuang, W.; Zheng, J., Ion clustering in aqueous solutions probed with vibrational energy transfer. *Proc. Nat. Acad. Sci. U.S.A.* **2011,** *108*, 4737-4742.

16. Sun, Z.; Zhang, W.; Ji, M.; Hartsock, R.; Gaffney, K. J., Contact Ion Pair Formation between Hard Acids and Soft Bases in Aqueous Solutions Observed with 2DIR Spectroscopy. *J. Phys. Chem. B* **2013,** *117*, 15306-15312.

17. van der Vegt, N. F. A.; Haldrup, K.; Roke, S.; Zheng, J.; Lund, M.; Bakker, H. J., Water-Mediated Ion Pairing: Occurrence and Relevance. *Chem. Rev.* **2016,** *116*, 7626-7641.

18. Fournier, J. A.; Carpenter, W.; De Marco, L.; Tokmakoff, A., Interplay of Ion–Water and Water–Water Interactions within the Hydration Shells of Nitrate and Carbonate Directly Probed with 2D IR Spectroscopy. *J. Am. Chem. Soc.* **2016,** *138*, 9634-9645.

19. Lim, J.; Park, K.; Lee, H.; Kim, J.; Kwak, K.; Cho, M., Nanometric Water Channels in Water-in-Salt Lithium Ion Battery Electrolyte. *J. Am. Chem. Soc.* **2018,** *140*, 15661-15667.

20. Lewis, N. H. C.; Zhang, Y.; Dereka, B.; Carino, E. V.; Maginn, E. J.; Tokmakoff, A., Signatures of Ion Pairing and Aggregation in the Vibrational Spectroscopy of Super-Concentrated Aqueous Lithium Bistriflimide Solutions. *J Phys Chem C* **2020,** *124*, 3470-3481.

21. Zhang, M.; Hao, H.; Zhou, D.; Duan, Y.; Wang, Y.; Bian, H., Understanding the Microscopic Structure of a "Water-in-Salt" Lithium Ion Battery Electrolyte Probed with Ultrafast IR Spectroscopy. *J Phys Chem C* **2020,** *124*, 8594-8604.

22. Suo, L.; Borodin, O.; Gao, T.; Olguin, M.; Ho, J.; Fan, X.; Luo, C.; Wang, C.; Xu, K., "Water-in-salt" electrolyte enables high-voltage aqueous lithium-ion chemistries. *Science* **2015,** *350*, 938-943.

23. Yamada, Y.; Usui, K.; Sodeyama, K.; Ko, S.; Tateyama, Y.; Yamada, A., Hydrate-melt electrolytes for high-energy-density aqueous batteries. *Nature Energy* **2016,** *1* (10), 16129.

24. Li, M.; Wang, C.; Chen, Z.; Xu, K.; Lu, J., New Concepts in Electrolytes. *Chem. Rev.* **2020,** *120*, 6783-6819.

25. Suo, L.; Borodin, O.; Wang, Y.; Rong, X.; Sun, W.; Fan, X.; Xu, S.; Schroeder, M. A.; Cresce, A. V.; Wang, F.; Yang, C.; Hu, Y.-S.; Xu, K.; Wang, C., "Water-in-Salt" Electrolyte Makes Aqueous Sodium-Ion Battery Safe, Green, and Long-Lasting. *Advanced Energy Materials* **2017,** *7*, 1701189.

26. Wang, F.; Borodin, O.; Gao, T.; Fan, X.; Sun, W.; Han, F.; Faraone, A.; Dura, J. A.; Xu, K.; Wang, C., Highly reversible zinc metal anode for aqueous batteries. *Nat. Mat.* **2018,** *17*, 543-549.

27. Zhao, J.; Li, Y.; Peng, X.; Dong, S.; Ma, J.; Cui, G.; Chen, L., High-voltage Zn/LiMn0.8Fe0.2PO4 aqueous rechargeable battery by virtue of “water-in-salt” electrolyte. *Electrochem. Commun.* **2016,** *69*, 6-10.

28. Johnston, C. T.; Agnew, S. F.; Schoonover, J. R.; Kenney, J. W.; Page, B.; Osborn, J.; Corbin, R., Raman Study of Aluminum Speciation in Simulated Alkaline Nuclear Waste. *Environmental Science & Technology* **2002,** *36*, 2451-2458.

29. Sipos, P., The structure of Al(III) in strongly alkaline aluminate solutions — A review. *J. Mol. Liq.* **2009,** *146*, 1-14.

30. Reynolds, J. G.; Cooke, G. A.; Herting, D. L.; Warrant, R. W., Salt Mineralogy of Hanford High-Level Nuclear Waste Staged for Treatment. *Industrial & Engineering Chemistry Research* **2013,** *52* (29), 9741-9751.

31. Soper, A. K., The radial distribution functions of water and ice from 220 to 673 K and at pressures up to 400 MPa. *Chem. Phys.* **2000,** *258*, 121-137.

32. Prendergast, D.; Galli, G., X-Ray Absorption Spectra of Water from First Principles Calculations. *Phys. Rev. Lett.* **2006,** *96*, 215502.

33. Marcus, Y.; Hefter, G., Ion Pairing. *Chem. Rev.* **2006,** *106*, 4585-4621.

34. Singh, M. B.; Dalvi, V. H.; Gaikar, V. G., Investigations of clustering of ions and diffusivity in concentrated aqueous solutions of lithium chloride by molecular dynamic simulations. *RSC Advances* **2015,** *5*, 15328-15337.

35. Pethes, I., The structure of aqueous lithium chloride solutions at high concentrations as revealed by a comparison of classical interatomic potential models. *J. Mol. Liq.* **2018,** *264*, 179-197.

36. Ibuki, K.; Bopp, P. A., Molecular dynamics simulations of aqueous LiCl solutions at room temperature through the entire concentration range. *J. Mol. Liq.* **2009,** *147*, 56-63.

37. Yuan, R.; Fayer, M. D., Dynamics of Water Molecules and Ions in Concentrated Lithium Chloride Solutions Probed with Ultrafast 2D IR Spectroscopy. *J. Phys. Chem. B* **2019,** *123*, 7628-7639.

38. Yuan, R.; Yan, C.; Fayer, M., Ion–Molecule Complex Dissociation and Formation Dynamics in LiCl Aqueous Solutions from 2D IR Spectroscopy. *J. Phys. Chem. B* **2018,** *122*, 10582-10592.

39. Andrews, S. S.; Boxer, S. G., Vibrational stark effects of nitriles I. Methods and experimental results. *J. Phys. Chem. A* **2000,** *104*, 11853-11863.

40. Williams, R. B.; Loring, R. F.; Fayer, M. D., Vibrational Dephasing of Carbonmonoxy Myoglobin. *J. Phys. Chem. B* **2001,** *105*, 4068-4071.

41. Bagchi, S.; Boxer, S. G.; Fayer, M. D., Ribonuclease S dynamics measured using a nitrile label with 2D IR vibrational echo spectroscopy. *J. Phys. Chem. B* **2012,** *116*, 4034-4042.

42. Fenn, E. E.; Wong, D. B.; Fayer, M. D., Water Dynamics in Small Reverse Micelles in Two Solvents: Two-Dimensional Infrared Vibrational Echoes with Two-Dimensional Background Subtraction. *J. Chem. Phys.* **2011,** *134*, 054512.

43. Steinel, T.; Asbury, J. B.; Zheng, J. R.; Fayer, M. D., Watching hydrogen bonds break: A transient absorption study of water. *J. Phys. Chem. A* **2004,** *108*, 10957-10964.

44. Rezus, Y. L. A.; Bakker, H. J., On the orientational relaxation of HDO in liquid water. *J. Chem. Phys.* **2005,** *123*, 114502.

45. Kwak, K.; Park, S.; Finkelstein, I. J.; Fayer, M. D., Frequency-frequency correlation functions and apodization in two-dimensional infrared vibrational echo spectroscopy: A new approach. *J. Chem. Phys.* **2007,** *127*, 124503.

46. Kwak, K.; Rosenfeld, D. E.; Fayer, M. D., Taking apart the two-dimensional infrared vibrational echo spectra: More information and elimination of distortions. *J. Chem. Phys.* **2008,** *128*, 204505.

47. Guo, Q.; Pagano, P.; Li, Y.-L.; Kohen, A.; Cheatum, C. M., Line shape analysis of two-dimensional infrared spectra. *J. Chem. Phys.* **2015,** *142*, 212427.

48. Bergström, P.-A.; Lindgren, J.; Kristiansson, O., An IR Study of the Hydration of ClO_4^-, NO_3^-, I^-, Br^-, Cl^-, and SO_4^{2-} Anions in Aqueous Solution. *J. Phys. Chem.* **1991,** *95*, 8575-8580.

49. Kropman, M. F.; Bakker, H. J., Vibrational relaxation of liquid water in ionic solvation shells. *Chem. Phys. Lett.* **2003,** *370*, 741-746.

50. Smith, J. D.; Saykally, R. J.; Geissler, P. L., The Effect of Dissolved Halide Anions on Hydrogen Bonding in Liquid Water. *J. Am. Chem. Soc.* **2007,** *129*, 13847-13856.

51. Kristiansson, O.; Lindgren, J., On the hydration of the F− anion in aqueous solution. *J. Mol. Struct.* **1988,** *177*, 537-541.

52. Stangret, J.; Gampe, T., Hydration Sphere of Tetrabutylammonium Cation. FTIR Studies of HDO Spectra. *J. Phys. Chem. B* **1999,** *103*, 3778-3783.

53. Nickolov, Z. S.; Miller, J. D., Water structure in aqueous solutions of alkali halide salts: FTIR spectroscopy of the OD stretching band. *J. Colloid Interface Sci.* **2005,** *287*, 572-580.

54. Kramer, P. L.; Giammanco, C. H.; Fayer, M. D., Dynamics of water, methanol, and ethanol in a room temperature ionic liquid. *J. Chem. Phys.* **2015,** *142*, 212408.

55. Giammanco, C. H.; Kramer, P. L.; Fayer, M. D., Ionic Liquid versus Li+ Aqueous Solutions: Water Dynamics near Bistriflimide Anions. *J. Phys. Chem. B* **2016,** *120*, 9997-10009.

56. Śmiechowski, M.; Gojło, E.; Stangret, J., Ionic Hydration in LiPF6, NaPF6, and KPF6 Aqueous Solutions Derived from Infrared HDO Spectra. *J. Phys. Chem. B* **2004,** *108*, 15938-15943.

57. Nam, D.; Lee, C.; Park, S., Temperature-dependent dynamics of water in aqueous NaPF6 solution. *Phys. Chem. Chem. Phys.* **2014,** *16*, 21747-21754.

58. Giammanco, C. H.; Kramer, P. L.; Wong, D. B.; Fayer, M. D., Water Dynamics in 1-Alkyl-3-methylimidazolium Tetrafluoroborate Ionic Liquids. *J. Phys. Chem. B* **2016,** *120*, 11523-11538.

59. Kenkre, V. M.; Tokmakoff, A.; Fayer, M. D., Theory of Vibrational Relaxation of Polyatomic Molecules in Liquids. *J. Chem. Phys.* **1994,** *101*, 10618-10629.

60. Timmer, R. L. A.; Bakker, H. J., Vibrational Förster Transfer in Ice Ih. *J. Phys. Chem. A* **2010,** *114*, 4148-4155.

61. Perakis, F.; Hamm, P., Two-dimensional infrared spectroscopy of neat ice Ih. *Phys. Chem. Chem. Phys.* **2012,** *14*, 6250-6256.

62. Zeng, Y.; Jia, Y.; Yan, T.; Zhuang, W., Binary structure and dynamics of the hydrogen bonds in the hydration shells of ions. *Phys. Chem. Chem. Phys.* **2021,** *23*, 11400-11410.

63. Laage, D.; Hynes, J. T., A Molecular Jump Mechanism of Water Reorientation. *Science* **2006,** *311*, 832-835.

64. Moilanen, D. E.; Fenn, E. E.; Lin, Y. S.; Skinner, J. L.; Bagchi, B.; Fayer, M. D., Water inertial reorientation: Hydrogen bond strength and the angular potential. *Proc. Nat. Acad. Sci. U.S.A.* **2008,** *105*, 5295-5300.

65. Kinosita, K.; Kawato, S.; Ikegami, A., Theory of Fluorescence Polarization Decay in Membranes. *Biophys. J.* **1977,** *20*, 289-305.

66. Kinosita, K.; Ikegami, A.; Kawato, S., On the wobbling-in-cone analysis of fluorescence anisotropy decay. *Biophys. J.* **1982,** *37*, 461-464.

67. Lipari, G.; Szabo, A., Effect of Librational Motion on Fluorescence Depolarization and Nuclear Magnetic-Resonance Relaxation in Macromolecules and Membranes. *Biophys. J.* **1980,** *30*, 489-506.

68. Hoffman, D. J.; Fica-Contreras, S. M.; Fayer, M. D., Amorphous polymer dynamics and free volume element size distributions from ultrafast IR spectroscopy. *Proc. Nat. Acad. Sci. U.S.A.* **2020,** *117*, 13949-13958.

69. Fica-Contreras, S. M.; Hoffman, D. J.; Pan, J.; Liang, C.; Fayer, M. D., Free Volume Element Sizes and Dynamics in Polystyrene and Poly(methyl methacrylate) Measured with Ultrafast Infrared Spectroscopy. *J. Am. Chem. Soc.* **2021,** *143*, 3583-3594.

70. Kubo, R., A Stochastic Theory of Line-Shape and Relaxation. In *Fluctuation, Relaxation and Resonance in Magnetic Systems*, Ter Haar, D., Ed. Oliver and Boyd: London, 1961.

71. Hamm, P.; Zanni, M. T., *Concepts and Methods of 2D Infrared Spectroscopy*. Cambridge University Press: Cambridge; New York, 2011.

72. Hoffman, D. J.; Fayer, M. D., CLS Next Gen: Accurate Frequency–Frequency Correlation Functions from Center Line Slope Analysis of 2D Correlation Spectra Using Artificial Neural Networks. *J. Phys. Chem. A* **2020,** *124*, 5979-5992.

73. Asbury, J. B.; Steinel, T.; Kwak, K.; Corcelli, S. A.; Lawrence, C. P.; Skinner, J. L.; Fayer, M. D., Dynamics of Water Probed with Vibrational Echo Correlation Spectroscopy. *J. Chem. Phys.* **2004,** *121*, 12431.

74. Asbury, J. B.; Steinel, T.; Stromberg, C.; Corcelli, S. A.; Lawrence, C. P.; Skinner, J. L.; Fayer, M. D., Water Dynamics: Vibrational Echo Correlation Spectroscopy and Comparison to Molecular Dynamics Simulations. *J. Phys.Chem. A* **2004,** *108*, 1107-1119.

75. Piskulich, Z. A.; Laage, D.; Thompson, W. H., On the role of hydrogen-bond exchanges in the spectral diffusion of water. *J. Chem. Phys.* **2021,** *154*, 064501.

76. Yamada, S. A.; Thompson, W. H.; Fayer, M. D., Water-anion hydrogen bonding dynamics: Ultrafast IR experiments and simulations. *J. Chem. Phys.* **2017,** *146*, 234501.

77. Błasiak, B.; Ritchie, A. W.; Webb, L. J.; Cho, M., Vibrational solvatochromism of nitrile infrared probes: beyond the vibrational Stark dipole approach. *Phys. Chem. Chem. Phys.* **2016,** *18*, 18094-18111.

78. Daly, C. A.; Berquist, E. J.; Brinzer, T.; Garrett-Roe, S.; Lambrecht, D. S.; Corcelli, S. A., Modeling Carbon Dioxide Vibrational Frequencies in Ionic Liquids: II. Spectroscopic Map. *J. Phys. Chem. B* **2016,** *120*, 12633-12642.

79. Lewis, N. H. C.; Iscen, A.; Felts, A.; Dereka, B.; Schatz, G. C.; Tokmakoff, A., Vibrational Probe of Aqueous Electrolytes: The Field Is Not Enough. *J. Phys. Chem. B* **2020,** *124*, 7013-7026.

Tables

Table 1. Observed lifetimes from fits to the population decays of the OD stretch of HOD in bulk water and in aqueous LiCl solutions.

Solution	t_w	t_a
1-4	1.3 ± 0.1	6.4 ± 0.1
1-5	1.1 ± 0.1	5.5± 0.1
1-6	1.0 ± 0.1	5.2 ± 0.1
Bulk water	1.8 ± 0.1	-

t_w - lifetime of the water-associated population; t_a - lifetime of the anion-associated population

Table 2. Fit parameters for the anisotropy of the OD stretch of HOD in bulk water and aqueous LiCl solutions using wobbling-in-a-cone analysis for restricted orientational relaxation.

Solution	t_1	t_c	D_c^{-1} (ps) [a,b]	θ_c (slope)[a]	$t_m = t_2$ (ps)	D_m^{-1} (ps)
1-4	1.6 ± 0.2	1.9 ± 0.2	34 ± 6	26 (0.11)	12 ± 1	72 ± 6
1-5	1.6 ± 0.1	2.0 ± 0.2	30 ± 4	28 (0.08)	10 ± 1	60 ± 6
1-6	1.8 ± 0.1	2.2 ± 0.2	28 ± 1	32 (0.04)	11 ± 1	66 ± 6
Bulk water	-	-	-	-	2.6 ± 0.1	15.6 ± 0.6

[a]average across all frequencies; [b] error bars are the standard deviation across all frequencies

Table 3. Complete FFCF parameters from the CLS decays and the linear absorption spectra[65] of the OD stretch of HOD in bulk water and in Aqueous LiCl solutions.

Sample	Γ (cm^{-1})	Δ_1 (cm^{-1})	τ_1 (ps)	Δ_2 (cm^{-1})	τ_2 (ps)
1-4	54 ± 5	35 ± 2	1.2 ± 0.1	43 ± 2	13 ± 1
1-5	55 ± 5	39 ± 2	1.1 ± 0.1	37 ± 2	13 ± 1
1-6	57 ± 4	41 ± 2	1.1 ± 0.1	32 ± 2	12 ± 1
Bulk water	67 ± 4	43 ± 2	0.4 ± 0.1	31 ± 2	1.7 ± 0.1

Figure Captions

Figure 1. Background subtracted and normalized linear absorption spectra of the OD stretch of HOD in bulk water and in aqueous LiCl solutions of concentrations, 1-4, 1-5, 1-6, and 1-16 (ion pairs to water). The three very high concentrations have almost identical spectra.

Figure 2. Normalized, frequency-dependent vibrational relaxation of the OD stretch of HOD in 1-5 LiCl aqueous solution.

Figure 3. Frequency-dependent population amplitudes (Lifetime Amplitude Spectra) at $t = 0$ of the water-associated and chloride-associated HOD populations determined from the biexponential curve fitting of the vibrational relaxation as described in the text.

Figure 4. Comparison of the OD stretch water-associated Lifetime Amplitude Spectrum of the 1-5 LiCl aqueous solution and bulk water.

Figure 5. Anisotropy decays of the OD stretch of HOD in aqueous LiCl solutions with concentrations, 1-4, 1-5, and 1-6 at the center frequency 2527 cm^{-1}.

Figure 6. Frequency-dependent cone angles determined from the wobbling-in-a-cone analysis of the measured anisotropy decays of HOD in aqueous LiCl solutions. Error bars are the standard deviation after analyzing three individual experiments for each concentration. Solid lines are a linear fit to the cone angles at each concentration.

Figure 7. Representative 2D IR spectra of the OD stretch of HOD in 1-5 aqueous LiCl solution at two waiting times, $T_w = 1$ ps and 10 ps. The spectral diffusion dynamics are obtained from analysis of the change in shape of the spectra with T_w.

Figure 8. CLS(T_w) decays (points) (spectral diffusion dynamics) and their corresponding fits (solid lines) for the OD stretch of HOD in aqueous LiCl solutions.

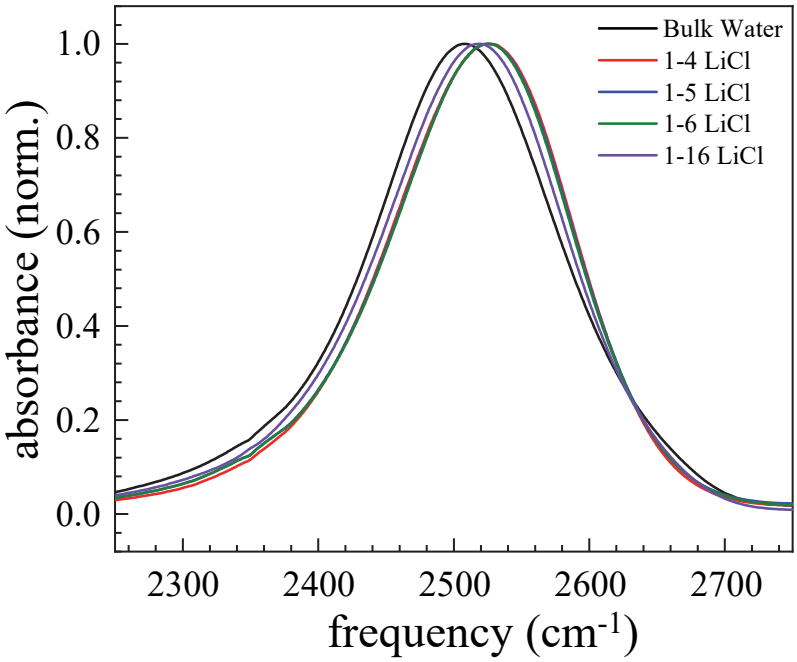
Bulk Water
1-4 LiCl
1-5 LiCl
1-6 LiCl
1-16 LiCl
absorbance (norm.)
1.0
0.8
0.6
0.4
0.2
0.0
2300
2400
2500
2600
2700
frequency (cm-1)

Figure 1.

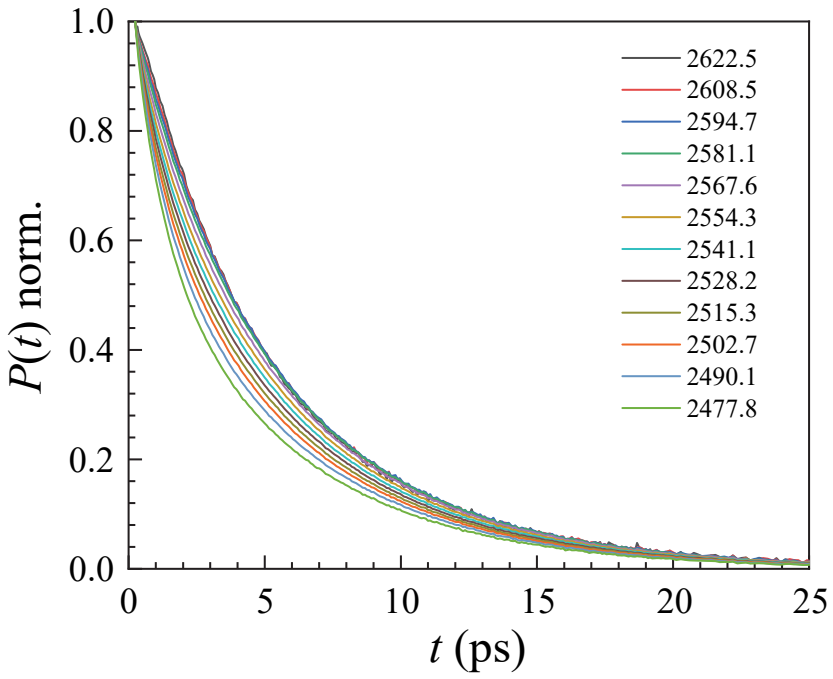
1.0
0.8
0.6
0.4
0.2
0.0
P(t) norm.
0
5
10
15
20
25
t (ps)
2622.5
2608.5
2594.7
2581.1
2567.6
2554.3
2541.1
2528.2
2515.3
2502.7
2490.1
2477.8

Figure 2.

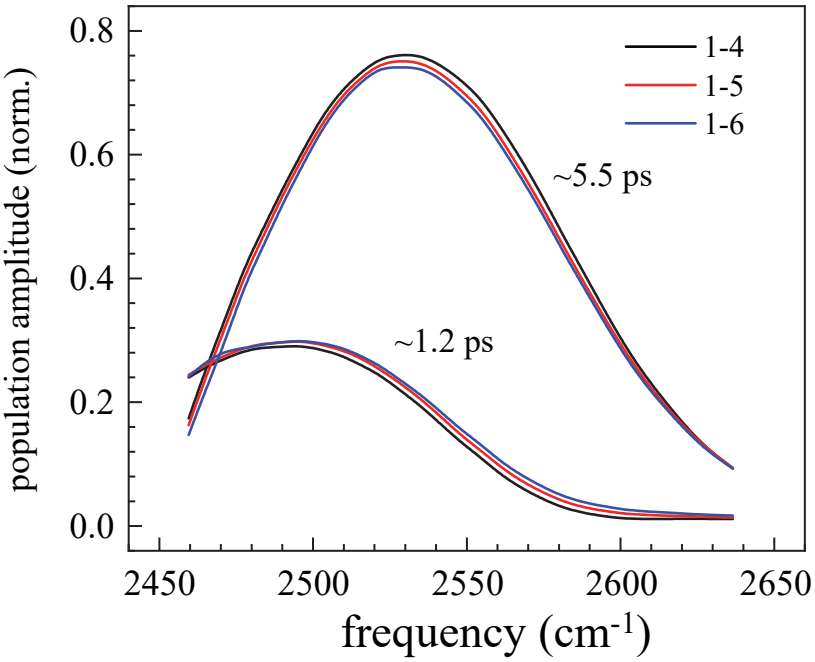
0.8
0.6
0.4
0.2
0.0
population amplitude (norm.)
2450
2500
2550
2600
2650
frequency (cm-1)
1-4
1-5
1-6
~5.5 ps
~1.2 ps

Figure 3.

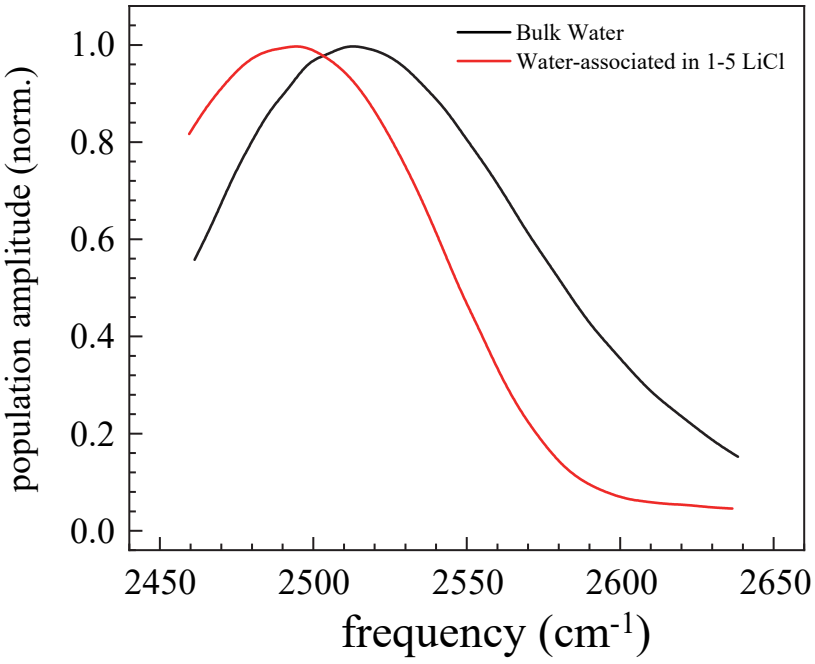
Bulk Water
Water-associated in 1-5 LiCl
population amplitude (norm.)
1.0
0.8
0.6
0.4
0.2
0.0
2450
2500
2550
2600
2650
frequency (cm-1)

Figure 4.

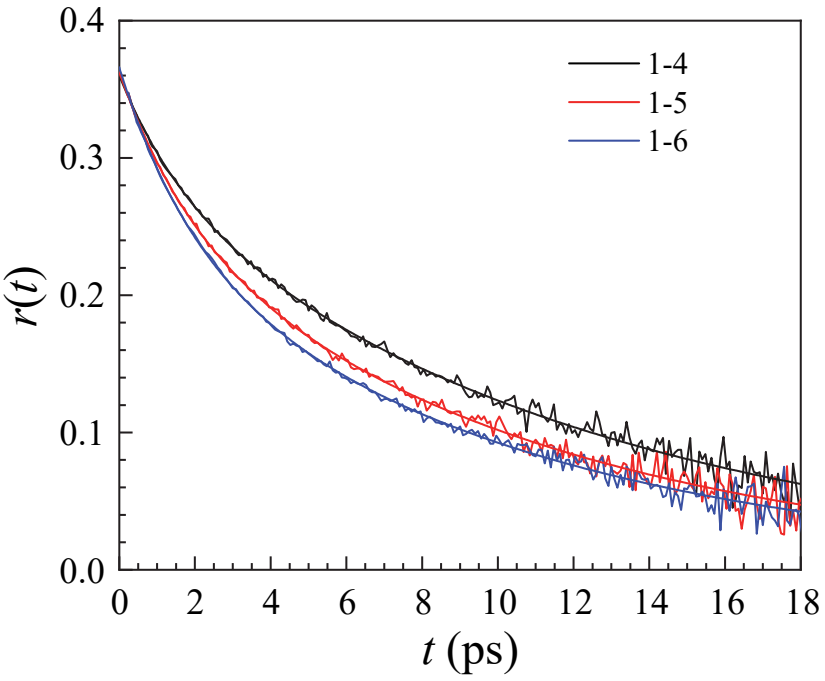

Figure 5.

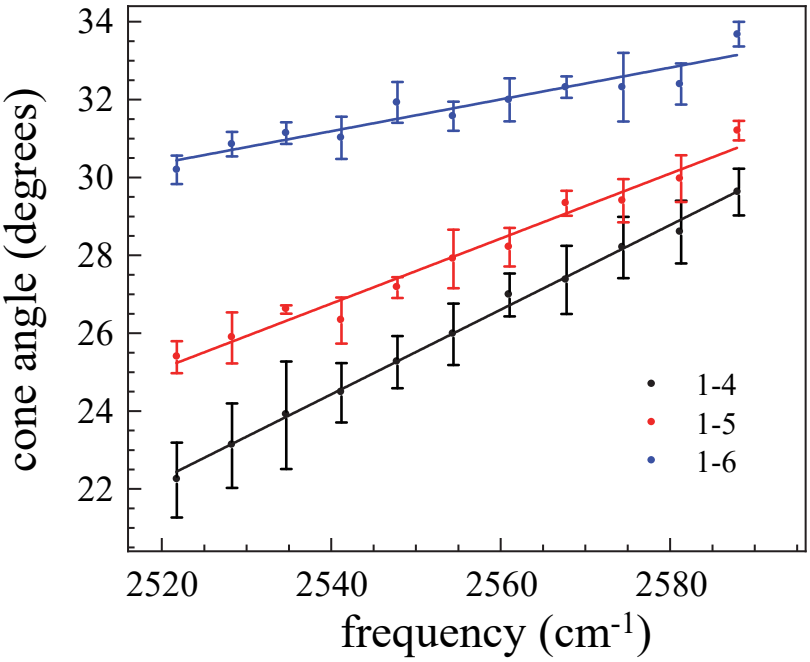
cone angle (degrees)
34
32
30
28
26
24
22
2520
2540
2560
2580
frequency (cm-1)
1-4
1-5
1-6

Figure 6.

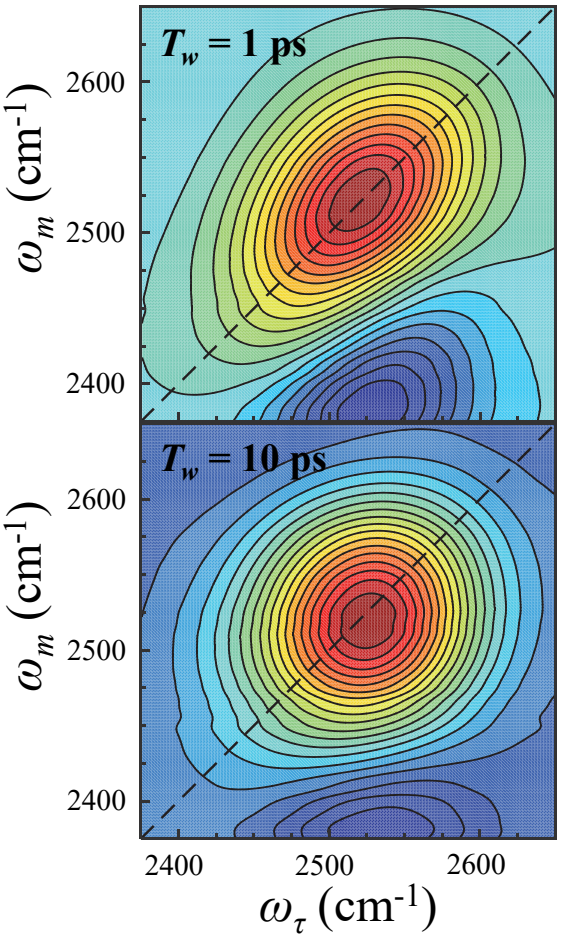

Figure 7.

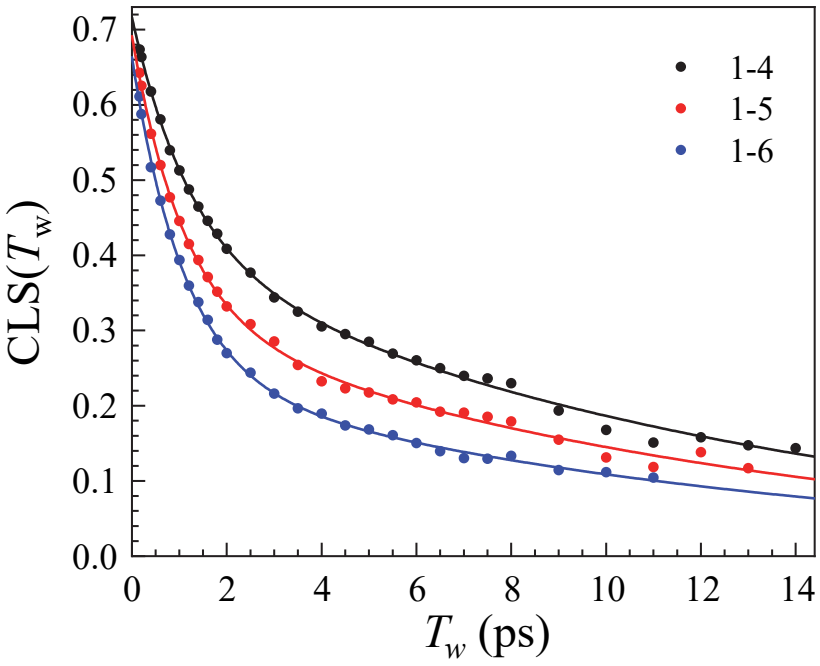

Figure 8.

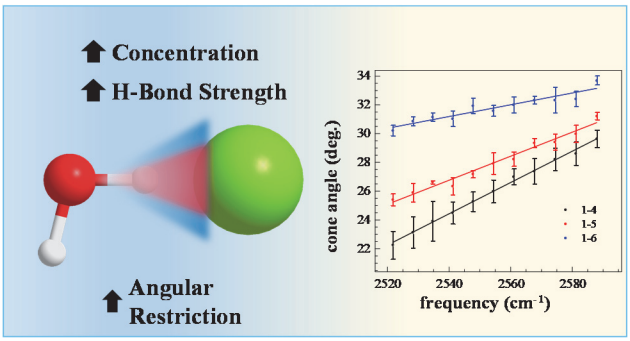
Concentration
H-Bond Strength
Angular Restriction
cone angle (deg.)
frequency (cm-1)
1-4
1-5
1-6

TOC Graphic